

## 镍离子与酵母乙醇脱氢酶的相互作用

尹国维<sup>1</sup> 尉薇<sup>1</sup> 徐佳<sup>1</sup> 李芝芬<sup>2</sup> 王保怀<sup>2</sup> 杜为红<sup>1,\*</sup>

(<sup>1</sup>中国人民大学化学系, 北京 100872; <sup>2</sup>北京大学化学与分子工程学院, 物理化学研究所, 北京 100871)

**摘要:** 不同体系中, 金属离子与蛋白以不同的结合方式相互作用. 酵母乙醇脱氢酶是一个含锌金属酶, 它可催化乙醇脱氢为乙醛的反应. 本文应用紫外-可见光谱、荧光光谱、差示扫描量热法等技术研究了二价镍离子与酵母乙醇脱氢酶的相互作用. 镍离子与酶结合后在 320 nm 出现了紫外吸收带, 同时荧光光谱反映了酶的构象变化, 紫外与荧光光谱均展现了结合过程的双相动力学. 镍离子与酶的相互作用导致了酶由四聚体向二聚体的解离; 在酶热变性过程中, 镍离子增加了乙醇脱氢酶的变性温度和变性焓. 研究工作揭示了镍离子与酶相互作用复杂和深层的作用机制.

**关键词:** 构象变化; 镍离子; 酵母乙醇脱氢酶; 相互作用

**中图分类号:** O641

## Interaction of Nickel (II) with *Yeast* Alcohol Dehydrogenase

YIN Guo-Wei<sup>1</sup> WEI Wei<sup>1</sup> XU Jia<sup>1</sup> LI Zhi-Fen<sup>2</sup> WANG Bao-Huai<sup>2</sup> DU Wei-Hong<sup>1,\*</sup>

(<sup>1</sup>Department of Chemistry, Renmin University of China, Beijing 100872, P. R. China;

<sup>2</sup>Institute of Physical Chemistry, College of Chemistry and Molecular Engineering, Peking University, Beijing 100871, P. R. China)

**Abstract:** The binding mode of metal ions with proteins is usually different in different systems. *Yeast* alcohol dehydrogenase (YADH) is a zinc containing metalloenzyme that catalyzes the fermentation reaction of alcohol to acetaldehyde. UV-Vis spectroscopy, fluorescence spectroscopy, and differential scanning calorimetry (DSC) were used to investigate the interaction of nickel (II) with *Yeast* alcohol dehydrogenase. The binding of Ni(II) to *Yeast* alcohol dehydrogenase shows a 320 nm UV absorbance band and the enzyme conformational change is reflected in the fluorescence data. Both UV-Vis and fluorescence spectra exhibit biphasic kinetics for the binding process. The interaction of Ni(II) with *Yeast* alcohol dehydrogenase causes the enzyme to transform from a tetramer to a dimer. The conformational change of the *Yeast* alcohol dehydrogenase results in an increase in the denaturation temperature and in a molar enthalpy change during the DSC process. This study reveals a complex but deep-seated mechanism for the interaction of Ni(II) with YADH.

**Key Words:** Conformational change; Nickel(II); *Yeast* alcohol dehydrogenase; Interaction

Metal ions are indispensable in kinds of biomacromolecules, especially in metalloproteins. They acts as cofactor or inhibitor in various proteins and in even engineered proteins<sup>[1-3]</sup>. *Yeast* alcohol dehydrogenase (YADH) is a metalloenzyme which catalyze the fermentation reaction of alcohol to acetaldehyde<sup>[4]</sup>. This

fermentation has been widely studied for its implications in wine and beer production<sup>[5-6]</sup>, and an increasing interest in its application for biotechnological processes of bioconversion of different organic wastes into ethanol to be used as solvent or fuel<sup>[7-8]</sup>. YADH is a tetramer (150 kD) with four subunits held together<sup>[9]</sup>.

Received: October 26, 2009; Revised: December 16, 2009; Published on Web: February 8, 2010.

\*Corresponding author. Email: whdu@chem.ruc.edu.cn; Tel: +86-10-62512660.

The project was supported by the National Key Basic Research Program of China (973) (2004CB719900), the National Natural Science Foundation of China(20633080), and Key Project of the Ministry of Education of China (108121).

国家重点基础研究发展规划项目(973) (2004CB719900), 国家自然科学基金(20633080)及教育部科技重点项目(108121)资助杜为红. 1997年9月-2000年7月在北京大学化学与分子工程学院攻读博士学位

Each subunit contains two zinc ions with one zinc ion located at the active site (catalytic zinc) and bound to two cysteines, one histidine and a water molecule. The other zinc ion bound to four cysteines and maintains the tertiary structure of the enzymes (structural zinc). The Zn(II) sites are conserved among ADHs from different species<sup>[10-14]</sup>.

The structure-activity relationships of ADHs are widely concerned in recent years. Evaluation of Hofmeister effects on ADH and other proteins indicated that the protein kinetics stability could be influenced by salt species and their concentration, and the thermodynamic parameters were also effected by some small molecules<sup>[15-16]</sup>. To improve the activity of ADH, some works focused on the transition metal substitution for zinc ions, and possible substrates and inhibitors were studied<sup>[12,17-18]</sup>. Moreover, the quantum mechanics method was used to show the kinetic isotope effects and enzyme motion<sup>[19]</sup>. The interaction of mithramycin and chromomycin with ADH were performed to check the binding affinity of the two anticancer antibiotics to bivalent cations, i.e. zinc ions in structural site or catalytic site<sup>[20-21]</sup>. This means the inhibitors of ADH are widely distributed. They include not only the classical reagent 4-methyl-pyrazole<sup>[12]</sup> and the anticancer compounds, but also different metal ions, such as copper<sup>[22]</sup> and bismuth<sup>[23]</sup>.

Among the bivalent cations, Ni(II) is reported to inhibit ADH in a mode of mixed type mechanism in previous study<sup>[22]</sup>, but little is known about the detailed information on Ni(II)-YADH interaction. In this paper, we have characterized the interaction and inhibition of Ni(II) to YADH. UV-Vis spectroscopy and fluorescence spectroscopy were used to investigate the binding process of Ni(II) and YADH. Ellman method<sup>[24]</sup> was carried out to determine the thiolate group binding to Ni(II). And the inhibition mechanism was studied by enzymatic reaction. Furthermore, the differential scanning calorimetry (DSC) and fast protein liquid chromatography (FPLC) were performed to evaluate the thermodynamic stability of protein.

## 1 Materials and methods

### 1.1 Samples

YADH and nicotinamide adenine dinucleotide (NAD) were purchased from Sigma-Aldrich Co. (USA). The enzyme was used without further purification. Nickelous acetate tetrahydrate, trihydroxymethyl aminomethane (Tris) and 5,5'-dithiobis(2-nitrobenzoic acid) (DTNB) were purchased from BBI company (USA). All other reagents were of analytical grade.

### 1.2 UV-Vis spectroscopy

UV-Vis spectroscopy was used to study the binding process of Ni(II) and YADH. The lyophilized powder of YADH was dissolved in  $2.0 \times 10^{-2} \text{ mol} \cdot \text{L}^{-1}$  Tris-HCl buffer at pH 8.0. Enzyme concentration was determined from the UV absorbance at 280 nm with an absorption coefficient ( $\epsilon_{280}$ ) of  $1.89 \times 10^5 \text{ mol}^{-1} \cdot \text{L} \cdot \text{cm}^{-1}$ <sup>[25]</sup>. The spectrum width was from 300 to 500 nm. 40 folds of Ni(II) ( $2.4 \times 10^{-4} \text{ mol} \cdot \text{L}^{-1}$ ) was added to  $6.0 \times 10^{-6} \text{ mol} \cdot \text{L}^{-1}$  YADH in  $2.0 \times 10^{-2} \text{ mol} \cdot \text{L}^{-1}$  Tris-HCl buffer at pH 8.0, 298.2 K.

The course of the reaction was monitored up to 300 min. All UV-Vis spectra were recorded on a Cary 50 spectrometer (Varian, USA) with thermostat holders at 298.2 K.

### 1.3 Fluorescence spectroscopy

The experiment was carried out on a Perkin Elmer LS55 fluorescence spectrometer. A solution of  $6.0 \times 10^{-7} \text{ mol} \cdot \text{L}^{-1}$  YADH reacted with 40 folds of Ni(II) in  $2.0 \times 10^{-2} \text{ mol} \cdot \text{L}^{-1}$  Tris-HCl buffer at pH 8.0, 298.2 K. The excitation wavelength was at 295 nm and the exit slit was set to 4 nm. The changes in emission intensities were obtained at regular time intervals. Each spectrum was corrected by blank subtraction using  $2.0 \times 10^{-2} \text{ mol} \cdot \text{L}^{-1}$  Tris-HCl buffer at pH 8.0.

### 1.4 Enzyme catalysis reaction

The concentrations of NAD<sup>+</sup> and NADH were determined using the extinction coefficients of  $6.22 \times 10^3 \text{ mol}^{-1} \cdot \text{L} \cdot \text{cm}^{-1}$  at 340 nm<sup>[26]</sup>. Enzyme activity was determined by the changes of initial rate of absorbance at 340 nm corresponding to the reduction of NAD<sup>+</sup> to NADH as previously reported<sup>[27]</sup>. The solution of YADH was incubated in the presence of excess of Ni(II) for 5 min. An aliquot was withdrawn and added to a solution containing  $1.5 \times 10^{-3} \text{ mol} \cdot \text{L}^{-1}$  NAD<sup>+</sup> and  $0.2 \text{ mol} \cdot \text{L}^{-1}$  EtOH. The final enzyme concentration was  $2.5 \times 10^{-9} \text{ mol} \cdot \text{L}^{-1}$  in solution. The initial rates ( $r_0$ ) of reaction were recorded at different concentrations of ethanol ranging from  $5.0 \times 10^{-3}$  to  $50.0 \times 10^{-3} \text{ mol} \cdot \text{L}^{-1}$ . The  $K_m$  and  $r_{max}$  for inhibited reactions and control were obtained from Lineweaver-Burk plots<sup>[28]</sup>.

$$r_0 = \frac{r_{max}[S]}{K_m + [S]} \quad (1)$$

$$\frac{1}{r_0} = \frac{K_m}{r_{max}} \cdot \frac{1}{[S]} + \frac{1}{r_{max}} \quad (2)$$

### 1.5 Thiolate group analysis of YADH

Ellman's method<sup>[24]</sup> was utilized to determine the free thiolate content (SH) of YADH before and after reacting with Ni(II). YADH was incubated with 100 folds of Ni(II) at 298.2 K, in  $2.0 \times 10^{-2} \text{ mol} \cdot \text{L}^{-1}$  Tris-HCl buffer, pH 8.0. A solution of DTNB ( $1.0 \times 10^{-2} \text{ mol} \cdot \text{L}^{-1}$ ) was added to the mixture. The final solution contained  $2.0 \times 10^{-6} \text{ mol} \cdot \text{L}^{-1}$  YADH,  $2.0 \times 10^{-4} \text{ mol} \cdot \text{L}^{-1}$  Ni(II) and  $5.0 \times 10^{-4} \text{ mol} \cdot \text{L}^{-1}$  DTNB. The reaction solution was incubated for 4 h until the absorbance at 412 nm did not change. The amount of generated *p*-nitrothiolate was determined using the extinction coefficient ( $\epsilon_{412}$ ) of  $1.42 \times 10^4 \text{ mol}^{-1} \cdot \text{L} \cdot \text{cm}^{-1}$ <sup>[29]</sup>.

### 1.6 Differential scanning calorimetry

Differential scanning calorimetry experiments were performed with a Setaram (Lyons, France) Micro DSC III calorimeter. The mixture of 40 folds of Ni(II) ( $2.4 \times 10^{-4} \text{ mol} \cdot \text{L}^{-1}$ ) and  $6.0 \times 10^{-6} \text{ mol} \cdot \text{L}^{-1}$  YADH was incubated for 12 h in  $2.0 \times 10^{-2} \text{ mol} \cdot \text{L}^{-1}$  Tris-HCl buffer at pH 8.0, 298.2 K. Then it was measured using the scanning rate of  $1.0 \text{ K} \cdot \text{min}^{-1}$ . The experimental temperature range was from 298.2 to 383.2 K. Temperature correction and baseline correction had been done before proceeding with the experiment. The sample volume was 0.8 mL. Tris-HCl buffer was used as the reference in all the three repeat experiments.

### 1.7 Fast protein liquid chromatography

A solution of  $10 \mu\text{mol} \cdot \text{L}^{-1}$  YADH was incubated with 40 folds of Ni(II) in  $100 \text{mmol} \cdot \text{L}^{-1}$  Tris-HCl at pH 8.0, 298 K. After 120 min, the mixture was injected to fast protein liquid chromatography (FPLC) system. The Tris-HCl buffer ( $100 \text{mmol} \cdot \text{L}^{-1}$ , pH 8.0) was used as an elution solvent. Chromatograms were recorded by monitoring the absorbance at 280 nm with a UV detector. Control experiments were performed in the absence of Ni(II). The molecular mass calibration curve for the column was obtained using bovine serum albumin (65 kDa) and cytochrome C (12 kDa) as standards.

## 2 Results

### 2.1 Binding of Ni(II) and YADH

The interaction of Ni(II) with YADH lead to a new UV-Vis absorption band (Fig.1A). With the mixture of 40 folds of Ni(II) to YADH solution, the absorbance centered at 320 nm increased gradually. This band was assigned as  $\text{S}^{-}\text{-Ni(II)}$  ligand-to-metal charge transfer (LMCT) transitions due to Ni(II) binding to the thiolate ligand. It could be used to monitor the progress of the reaction between Ni(II) and YADH. Kinetics of the reaction was described by the dependence of absorption spectrum on time (Fig.1B). It was characterized by an initial rapid increase in absorbance, then a progressive increase for the duration. The two-kinetic steps could be resolved, which obey first-order kinetics

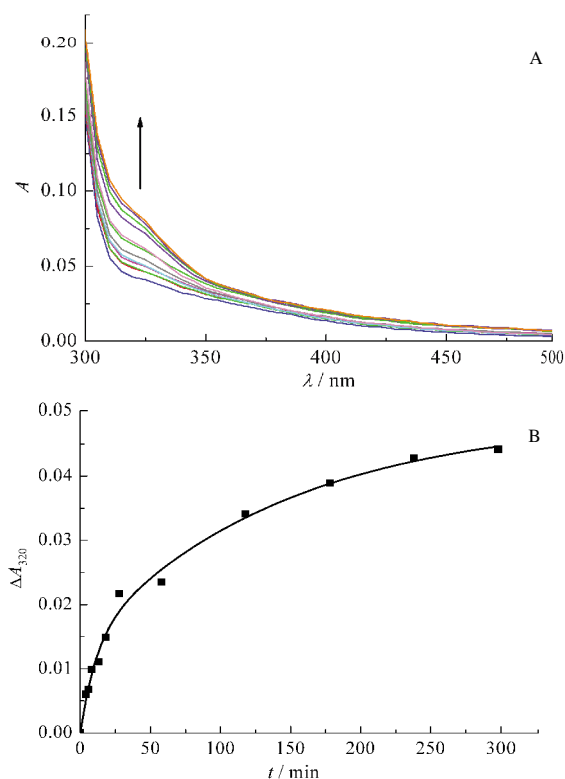


**Fig.1 (A) Time scale of absorption spectrum, (B) kinetics of the reaction of Ni(II) to YADH at 320 nm**

solution containing YADH ( $6.0 \times 10^{-6} \text{mol} \cdot \text{L}^{-1}$ ) and 40 folds of Ni(II) in  $2.0 \times 10^{-2} \text{mol} \cdot \text{L}^{-1}$  Tris-HCl at pH 8.0, 298.2 K; the broad band centered at 320 nm in Fig.1A indicating formation of Ni(II)-S (thiolate) bonds, reaction times from bottom to top: 0, 2, 4, 6, 8, 10, 15, 20, 50, 80, 145, and 300 min.

and fit to a bi-exponential growth using the non-linear least square method:

$$A(t) = A_1 \exp(-k_1 t) + A_2 \exp(-k_2 t) \quad (3)$$

where  $k_1$  and  $k_2$  are the rate constants of the two kinetic phases,  $A_1$  and  $A_2$  are the corresponding amplitudes that show the contribution of the individual kinetic phases to the observed change in absorbance. The rate constant  $k_1$ , was measured to be  $0.091 \text{min}^{-1}$ , and contributed 28% to the whole reaction<sup>[23]</sup>. And the rate constant  $k_2$ , had a value of  $6.9 \times 10^{-3} \text{min}^{-1}$  representing the rest of the reaction.

### 2.2 Conformational change in YADH due to the binding of Ni(II)

Fluorescence spectroscopy is widely used in protein conformational investigation since the tryptophan and tyrosine residues can produce intrinsic fluorescence<sup>[30]</sup>. YADH has five tryptophan residues in each subunit. These residues produce an intrinsic fluorescence for YADH at 340 nm. With the mixture of 40 folds of Ni(II) to YADH solution, the fluorescence emission intensity decreased obviously (Fig.2A). It revealed that conformational changes occurred in YADH upon Ni(II) binding. The decrease of YADH intensity *versus* time was also in a biphasic process and could be fitted by a two-exponential function as used in UV data processing (Fig.2B). The rate constant  $k_1$  for the fast step was measured to be  $0.48 \text{min}^{-1}$ , which contributed to 21% of the reaction, while

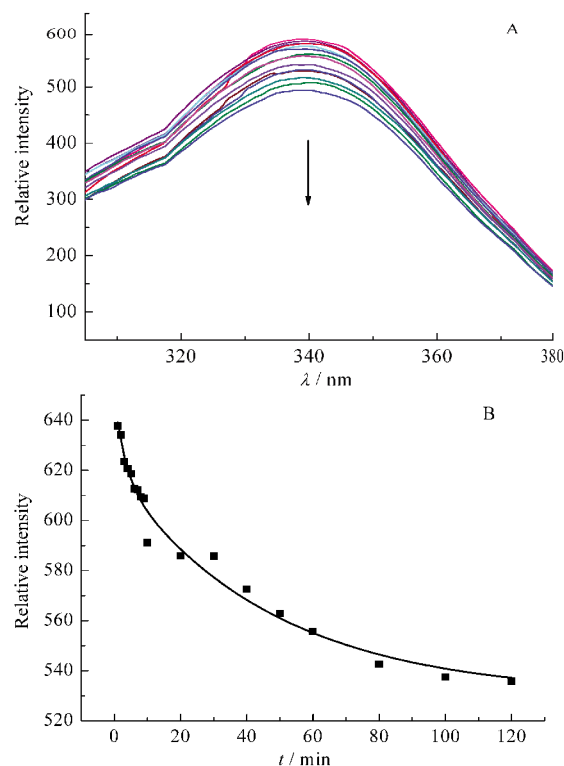


**Fig.2 (A) Time scale of fluorescence emission spectra with an excitation wavelength of 295 nm, (B) kinetics of the reaction of Ni(II) to YADH at 340 nm emission intensity**

solution containing YADH ( $6.0 \times 10^{-7} \text{mol} \cdot \text{L}^{-1}$ ) and 40 folds of Ni(II) in  $2.0 \times 10^{-2} \text{mol} \cdot \text{L}^{-1}$  Tris-HCl at pH 8.0, 298.2 K; reaction time from top to bottom: 0, 1, 2, 3, 4, 5, 6, 7, 8, 9, 10, 20, 30, 40, 50, 60, 80, 100, and 120 min

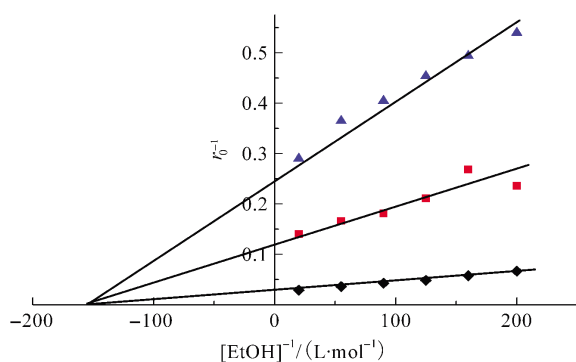


**Fig.3 Lineweaver-Burk plots of the enzyme catalysis reaction**

The solution is composed of  $2.5 \times 10^{-9} \text{ mol} \cdot \text{L}^{-1}$  YADH and  $1.5 \times 10^{-3} \text{ mol} \cdot \text{L}^{-1}$   $\text{NAD}^+$  at 298.2 K,  $2 \times 10^{-2} \text{ mol} \cdot \text{L}^{-1}$  Tris-HCl, pH 8.0.  $K_m$  for control reaction ( $\blacklozenge$ ) was found to be  $8.37 \times 10^{-3} \text{ mol} \cdot \text{L}^{-1}$ . The value is in agreement with that of control in the presence of 60 ( $\blacksquare$ ) and 240 ( $\blacktriangle$ ) folds of Ni(II)

the rate constant  $k_2$  for the slow step had a value of  $2.1 \times 10^{-2} \text{ min}^{-1}$  that represented the rest of the reaction. The rates are slightly higher than the corresponding values obtained from UV-Vis spectroscopy.

### 2.3 Inhibition of Ni(II) to YADH activity

Based on the interaction study of YADH and Ni(II), we measured the rate of ethanol oxidation catalyzed by YADH at different substrate concentrations in the presence of Ni (II). The kinetics of enzyme catalysis reaction can be described by a Michaelis-Menten model. In the present work, the  $K_m$  and  $r_{\text{max}}$  were calculated to be of  $8.3 \times 10^{-3} \text{ mol} \cdot \text{L}^{-1}$  and  $41.48 \text{ OD} \cdot \text{s}^{-1}$  (OD: optical density) respectively for the uninhibited control reaction, which were acceptable for further enzymatic inhibition analysis<sup>[31]</sup> (Fig. 3). And the  $K_m$  values obtained in the presence of 60 folds and 240 folds of Ni (II) were almost the same as in the absence of Ni(II). However, the  $r_{\text{max}}$  decreased significantly due to the increase of Ni(II). The Lineweaver-Burk plots showed a typical mode of noncompetitive inhibition<sup>[28]</sup>.

### 2.4 Thiolate group analysis of YADH

The free thiolate contents were determined using DTNB by Ellman's method so as to investigate whether Ni(II) binds to free Cys residues of YADH. The amount of generated *p*-nitrothiolate

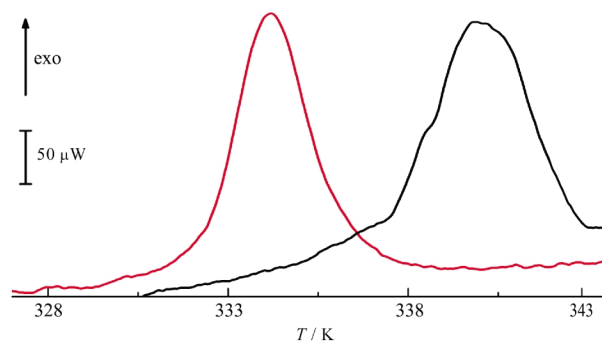


**Fig.4 DSC curves for pure YADH in the presence and absence of Ni(II)**

In the absence of Ni(II), the onset temperature is measured at  $(330.0 \pm 0.2) \text{ K}$  (left curve), the corresponding value in the presence of 40 folds of Ni(II) is measured at  $(335.8 \pm 0.3) \text{ K}$  (right curve)

was determined using the absorbance at 412 nm as described in the experimental section<sup>[29]</sup>. Totally, 36 free Cys residues are found in each YADH subunit after treatment with dithiolthreitol (DTT)<sup>[32]</sup>. 19 free SH groups in the native enzyme were determined in the present work. After incubation with 100 folds of Ni(II) for 4 h at pH 8.0 Tris-HCl buffer, 298.2 K, the number of free thiolate groups was determined to be 15. Therefore, there is one free thiol group loss in each subunit of YADH compared to its intact form.

### 2.5 Thermal denaturation of YADH upon binding of Ni(II)

The DSC method provided significant information about the thermodynamic properties of protein molecules, and the influence of molecular interactions on the stability of proteins and nucleic acids<sup>[33-34]</sup>. The denaturation experiment of YADH by DSC started from 298.2 to 383.2 K and returned from 383.2 to 298.2 K. YADH showed an irreversible denaturation process (Fig.4). There was an exothermic peak at  $(330.0 \pm 0.2) \text{ K}$  (onset point), which was very similar as reported<sup>[6]</sup>. The molar enthalpy change of denaturation of  $(-7.6 \pm 0.5) \times 10^4 \text{ kJ} \cdot \text{mol}^{-1}$  was too large for conformational change and possibly due to protein sedimentation. Addition of Ni (II) resulted in the increase of molar enthalpy

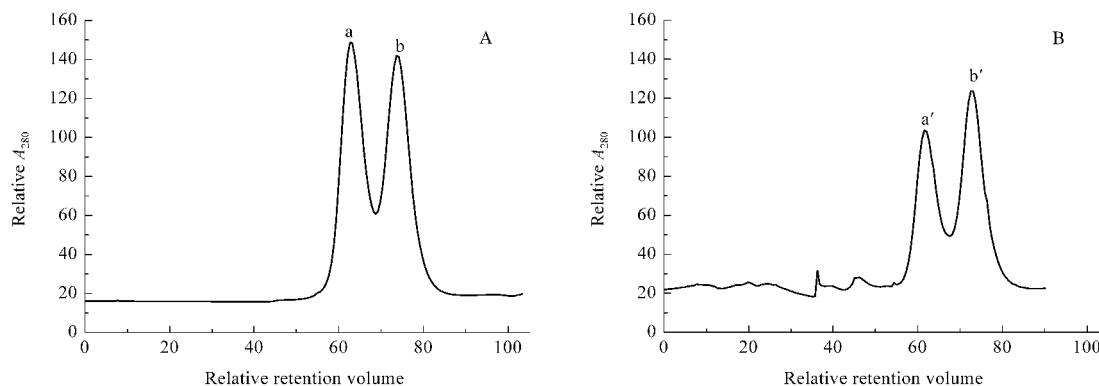


**Fig.5 FPLC profiles of YADH after incubation with Ni(II)**

(A) native YADH, (B) YADH with 40 folds of Ni(II) incubation after 120 min; A solution of ca  $10 \mu\text{mol} \cdot \text{L}^{-1}$  YADH was incubated with 40 folds of Ni(II) in  $100 \text{ mmol} \cdot \text{L}^{-1}$  Tris-HCl, pH 8.0

change and denaturation temperature to  $(-8.9 \pm 0.3) \times 10^4$  kJ·mol<sup>-1</sup> and  $(335.8 \pm 0.3)$  K (onset point), respectively.

### 2.6 Fast protein liquid chromatography study

Metal ions are known to affect signal transduction and protein-protein interaction. We carried out this experiment in order to demonstrate whether Ni(II) interferes with the quaternary structure of the native YADH. After loading YADH solution into the column, the relative retention volume value was observed at 62.9 and 74.0, respectively. Peak a in Fig.5A corresponds to a 150 kDa species based on the mass calibration curve, while peak b corresponds to a component with a molecular mass about 75 kDa. Therefore, they can be assigned to the tetramer and dimer of YADH respectively. The existence of dimer might be from conformational equilibrium of ADH in solution. After incubation with Ni(II), the peak at 62.9 decreased in its relative intensity obviously (Fig.5B). While the peak at 74.0 increased in its relative intensity gradually. This suggests that part of tetrameric YADH dissociates into a dimer, presumably due to the binding of Ni(II) to the enzyme.

### 3 Discussion

YADH is a classical enzyme which contains two zinc (II) ions in each subunit, one in its active site and another in auxiliary site. The enzymatic activity has been reported to be inhibited by some metal ions at various conditions<sup>[18,22-23]</sup>. Ni(II) is an important transition metal that takes part in many biological processes<sup>[34]</sup>. In the present work, we reported the interaction of Ni(II) with YADH. The results show that Ni(II) can bind to YADH and change the conformation of YADH.

UV-Vis spectroscopy reveals that the binding of Ni(II) leads to the appearance of 320 nm absorbance band. The time scale shows two kinetics steps for Ni(II) binding. The rate constants are less than those obtained from fluorescence spectrum, which indicate that the conformational change is prior to the binding of Ni(II) to thiolate group of ADH.

Although the inhibition of Ni(II) on recombinant ADH exhibits a mixed type mechanism<sup>[22]</sup>, our data show a noncompetitive inhibition in the enzyme catalysis reaction at the beginning of Ni(II) binding. Since the binding process is time dependent and the enzymatic conformation changes gradually, the conclusive mechanism of inhibition is inenarrable. The complexity might be induced by the anion effect compared with previous result<sup>[22]</sup>, since anion plays a key role in enzymatic activity and protein stability<sup>[12,15,35]</sup>. The used sample in this case was nickelous acetate tetrahydrate, and further work is needed to compare the binding mechanism by different Ni(II) compounds in order to make it clear.

Ni(II) binding could lead to the dissociation of YADH from tetramer to dimer, which is verified by FPLC experiments. The relative stability of dimer indicates that YADH could be described as a "Tetramer of dimers" with two identical interfaces. Hence in the DSC process, the binding of Ni(II) induces YADH in a higher denaturation temperature and molar enthalpy change.

And we might conclude that conformational change arisen from Ni(II) binding influences the path of YADH thermal denaturation.

Metal ions inhibition of YADH reveals various but exciting results. The investigation on interaction of Ni(II) and YADH makes a whole profile of the metal binding than ever. And it provides more information to understand metal-protein interaction.

### References

- 1 Lu, Y.; Berry, S. M.; Pfister, T. D. *Chem. Rev.*, **2001**, **101**: 3047
- 2 Xu, K.; Yang, X. D.; Wang, K. *Chem. J. Chin. Univ.*, **2008**, **29**: 2525 [徐 崑, 杨晓达, 王 夔. 高等学校化学学报, **2008**, **29**: 2525]
- 3 Huang, Z. X. *Prog. Chem.*, **2002**, **14**: 318 [黄仲贤. 化学进展, **2002**, **14**: 318]
- 4 Ramaswamy, S.; Kratzer, D. A.; Hershey, A. D.; Rogers, P. H.; Arnone, A.; Eklund, H.; Plapp, B. V. *J. Mol. Biol.*, **1994**, **235**: 777
- 5 Blandino, A.; Caro, I.; Cantero, D. *Biotechnol. Lett.*, **1997**, **19**: 651
- 6 Onnela, M. L.; Suihko, M. L.; Penttil, M.; Keraen, S. *J. Biotechnol.*, **1996**, **49**: 101
- 7 Fernandez, M. R.; Biosca, J. A.; Martinez, M. C.; Achkor, H.; Farres, J.; Pares, X. *Adv. Exp. Med. Biol.*, **1997**, **414**: 373
- 8 Lortie, R.; Fassouane, A.; Laval, J. M.; Bourdillon, C. *Biotechnol. Bioeng.*, **1992**, **39**: 157
- 9 Vanni, A.; Pessione, E.; Anfossi, L.; Baggiani, C.; Cavaletto, M.; Gulmini, M.; Giunta, C. *J. Mol. Catal. B: Enzym.*, **2000**, **9**: 283
- 10 Magonet, E.; Hayen, P.; Delforge, D.; Delaive, E.; Remacle, J. *Biochem. J.*, **1992**, **287**: 361
- 11 Meijers, R.; Adolph, H. W.; Dauter, Z.; Wilson, K. S.; Lamzin, V. S.; Cedergren-Zeppezauer, E. S. *Biochemistry*, **2007**, **46**: 5446
- 12 Reimers, M. J.; Hahn, M. E.; Tanguay, R. L. *J. Biol. Chem.*, **2004**, **279**: 38303
- 13 Rubach, J. K.; Plapp, B. V. *Biochemistry*, **2002**, **41**: 15770
- 14 Winberg, J. O.; Brendskag, M. K.; Sylte, I.; Lindstad, R. I.; McKinley-McKee, J. S. *J. Mol. Biol.*, **1999**, **294**: 601
- 15 Broering, J. M.; Bommarius, A. S. *J. Phys. Chem. B*, **2005**, **109**: 20612
- 16 Nath, S.; Satpathy, G. R.; Mantri, R.; Deep, S.; Ahluwalia, J. C. *J. Chem. Soc. Faraday Trans.*, **1997**, **93**: 3351
- 17 Kleifeld, O.; Rulisek, L.; Bogin, O.; Frenkel, A.; Havlas, Z.; Burstein, Y.; Sagi, I. *Biochemistry*, **2004**, **43**: 7151
- 18 Vanni, A.; Anfossi, L.; Pessione, E.; Giovannoli, C. *Int. J. Biol. Macromol.*, **2002**, **30**: 41
- 19 Billeter, S. R.; Webb, S. P.; Agarwal, P. K.; Iordanov, T.; Hammes-Schiffer, S. *J. Am. Chem. Soc.*, **2001**, **123**: 11262
- 20 Das, S.; Devi, P. G.; Pal, S.; Dasgupta, D. *J. Bio. Inorg. Chem.*, **2005**, **10**: 25
- 21 Devi, P. G.; Chakraborty, P. K.; Dasgupta, D. *J. Biol. Inorg. Chem.*, **2009**, **14**: 347
- 22 Cavaletto, M.; Pessione, E.; Vanni, A.; Giunta, C. *J. Biotechnol.*,

- 2001, **84**: 87
- 23 Jin, L.; Szeto, K. Y.; Zhang, L.; Du, W. H.; Sun, H. Z. *J. Inorg. Biochem.*, **2004**, **98**: 1331
- 24 Ellman, G. L. *Arch. Biochem. Biophys.*, **1959**, **82**: 70
- 25 Buhner, M.; Sund, H. *Eur. J. Biochem.*, **1969**, **11**: 73
- 26 Tkachenko, A. G.; Winston, G. W. *Arch. Biochem. Biophys.*, **2000**, **380**: 165
- 27 Vallee, B. L.; Hoch, F. L. *Proc. Natl. Acad. Sci. U.S.A.*, **1955**, **41**: 327
- 28 Wang, J. Y.; Zhu, S. G.; Xu, C. F. *Biochemistry*. Beijing: Higher Education Press, **2002**: 351–383 [王镜岩, 朱圣庚, 徐长法. 生物化学. 北京: 高等教育出版社, 2002: 351–383]
- 29 Riddles, P. W.; Blakeley, R. L.; Zerner, B. *Meth. Enzymol.*, **1983**, **91**: 49
- 30 Jornvall, H.; Eklund, H.; Branden, C. I. *J. Biol. Chem.*, **1978**, **253**: 8414
- 31 Dickinson, F. M.; Monger, G. P. *Biochem. J.*, **1973**, **131**: 261
- 32 Harris, I. *Nature*, **1964**, **203**: 30
- 33 Du, W. H.; Han, W.; Li, Z. F.; Wang, B. H. *Thermochim. Acta*, **2000**, **359**: 55
- 34 Du, W. H.; Wang, L.; Li, J.; Wang, B. H.; Li, Z. F.; Fang, W. H. *Thermochim. Acta*, **2007**, **452**: 31
- 35 Buhler, R.; Von Wartburg, J. P. *FEBS Lett.*, **1984**, **178**: 249